PCCP

Accepted Manuscript

ROYAL SOCIETY OF CHEMISTRY

www.rsc.org/pccp

Journal Name

RSCPublishing

COMMUNICATION

Ferroelectric photocatalyst for enhancing hydrogen evolution: Polarized particulate suspension

Cite this: DOI: 10.1039/x0xx00000x

Sangbaek Park,[a] Chan Woo Lee,[a] Min Gyu Kang,[b] Sanghyeon Kim,[a] Hae Jin Kim,[a] Ji Eon Kwon,[a] Soo Young Park,[a] Jong Yun Kang,[bc] Kug Sun Hong*[a] and Ki Tae Nam*[a]

Received 00th January 2012,
Accepted 00th January 2012

DOI: 10.1039/x0xx00000x

www.rsc.org/

A particle-based photocatalyst with a permanent internal field by corona poling method is presented as a novel approach to enhance the hydrogen evolution reaction in a particulate-suspension system. Photocatalytic activity of $K_{0.5}Na_{0.5}NbO_3$ was significantly improved by 7.4 times after the polarization.

Semiconductor-based artificial photosynthesis, especially the production of hydrogen from water, is considered to be an ideal, renewable energy resource for the future.[1, 2] The best quantum yield (QY) in a wide-band-gap photocatalyst that has been reported thus far is 56% for $NiO_x/NaTaO_3$:La at 270 nm;[3] in visible-light-sensitized photocatalyst, the highest QY is 2.5% for $Rh_{2-x}Cr_xO_3$/GaN:ZnO solid solution at 420 – 440 nm.[4, 5] Although energy-band modulations have been extensively studied,[6, 7] a significant QY cannot be achieved simply by tuning the conduction- and valence-band positions. Nano-interface engineering can promote surface catalytic reactions by increasing the proportion of depletion region in a semiconductor by reducing the particle dimension.[8] However, non-stoichiometry with oxygen or cation vacancies introduces considerable surface defects, which act as recombination centers for photo-generated carriers.[9] Deposition of cocatalysts is also an effective method of creating modifications for photocatalysis, providing low overpotential and highly catalytically active sites.[10] However, no satisfactorily cost-effective approach has yet been found because most suitable cocatalysts consist of precious metals, such as Pt, Au and Ag, or their oxides.[11] In the study presented here, we proposed a feasible strategy for further increasing photocatalytic activity by imposing a persistent internal polarization on each semiconductor particle.

Ferroelectric materials have spontaneous polarization, which can be reoriented between equivalent domain states by an applied electric field.[12-14] It is well known that the polarization of ferroelectrics affects the electrical behavior of photoinduced charge carriers.[15] In $BiFeO_3$ film, large photocurrent flow arises when light is applied to illuminate the positively charged (+) surface.[16] This photocurrent is caused by polarization-induced surface charge and the migration of oxygen vacancies on the (+) surface, which reduces the Schottky barrier and promotes the transfer of electrons to the electrolyte. In a $BaTiO_3$[17, 18] and PSZT[19] bulk pellet, the acceleration of the separation of electrons and holes by polarization has been demonstrated via the spatial selectivity of the photo reduction and oxidation reactions that occur on the (+) and (-) surfaces, respectively. Surprisingly, when coated on the (+) surface of PZT substrate, WO_3 can produce hydrogen, despite the inadequate band position.[15] This phenomenon is attributed to the fact that the photovoltage becomes several orders of magnitude larger than the band gap in ferroelectric materials, while the photovoltage in semiconducting materials is typically below 1 V. These phenomena are analogous to the behavior of charge carriers under an electric field. Therefore, a material with both ferroelectric and photocatalytic properties, a ferroelectric photocatalyst, enables the creation of a polarized photocatalyst; it can provide an electric bias effect on each particle. However, to date, there is seldom report about the effect of polarization on photocatalytic hydrogen evolution reaction (HER) in a Particulate suspension (PS) system because applying polarity on a powder is difficult. Very recently, Dunn et al fabricated the $BaTiO_3$ powder with a high tetragonal content by simple thermal treatment and showed that it has a 3-fold higher photocatalytic degradation rate of Rhodamine B dye compared to predominantly cubic material due to ferroelectricity of the tetragonal phase.[20] Some researchers reported that the ferroelectric domain affects the activity of $NaNbO_3$-related film and particles by control of synthesis method.[21, 22] Inspired by this pioneer studies, we designed a further broad and general approach for imposing an internal field on each particle and investigated the effect of polarization on photocatalytic activity systematically.

Herein, we report that the photocatalytic HER activity increases in a polarized PS system. The key factor is to introduce the corona-poling method, which has previously been used for the poling of film or polymer, for the poling of powder. In this manner, a general

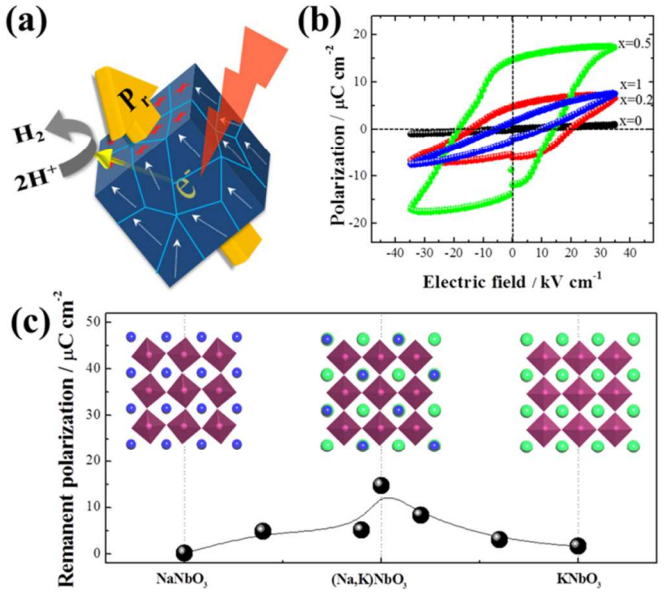

Fig. 1 (a) Scheme of polarization behavior for a semiconducting powder. (b) Hysteresis curves of $Na_{1-x}K_xNbO_3$ solid-solution ceramics. (c) Remanent polarization and crystal structure for (Na,K)NbO_3 solid-solution compounds.

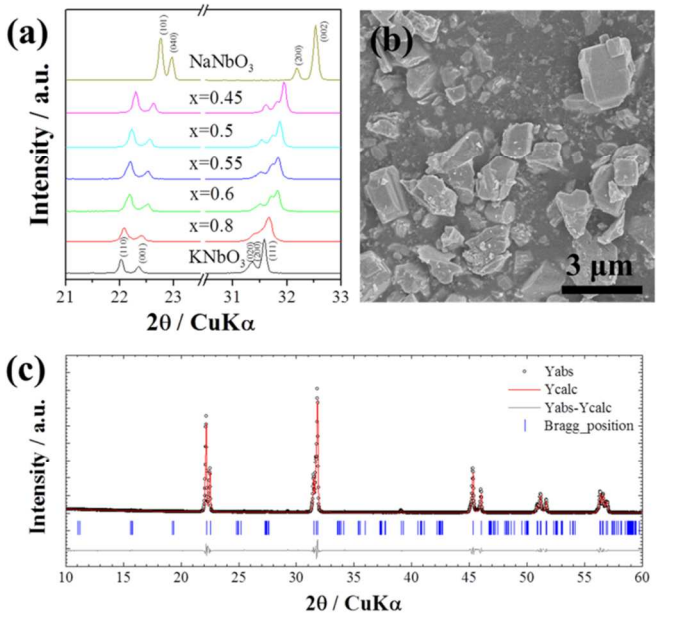

Fig. 2 (a) XRD graphs of $K_xNa_{1-x}NbO_3$ samples with different Na substitutions. (b) SEM image of $Na_{0.5}K_{0.5}NbO_3$ powder. (c) Rietveld-refined XRD patterns for $K_{0.5}Na_{0.5}NbO_3$ powder. The circles represent measured points, and the solid red line represents Rietveld-refined data. The bottom gray line shows the difference between the measured and refined data. The marked 2θ positions represent the allowed Bragg peaks.

and systematic route was developed that can impose internal electric fields upon all types of ferroelectric photocatalyst powders. As a proof of concept, $K_xNa_{1-x}NbO_3$ solid solution was selected as such a ferroelectric photocatalyst (Fig. 1a). Under optimum conditions, $K_{0.5}Na_{0.5}NbO_3$ exhibits superb catalytic activity after polarization, 7.4 times higher than that of the non-polarized material.

$K_xNa_{1-x}NbO_3$ powders were synthesized using a conventional solid-state method. To investigate the ferroelectric property of $K_xNa_{1-x}NbO_3$, the obtained powders were pressed into pellets and then sintered at a temperature close to the melting point. The prepared pellets achieved a high density of above 90%. Fig. 1b shows a well-saturated *P–E* hysteresis loop of NKN ceramics. The remanent polarization (P_r) and the coercive field (E_c) were 14.7 μC cm^{-2} and 14.0 kV cm^{-1}, respectively, consistent with previous values.[23-25] This result indicates that $K_xNa_{1-x}NbO_3$ exhibits ferroelectric properties as reported.[26] As shown in Fig. 1c, P_r of a $NaNbO_3$-$KNbO_3$ solid solution reaches its maximum value at 50 mol% Na dopant content, indicating that NKN has its highest ferroelectric property in solid solution. The origin of the ferroelectric property can be explained as a distortion in the crystal structure. As seen in the crystal structure of $KNbO_3$, a rhombohedral distortion of the center ions (Nb^{5+}) in the perovskite structure is found because of the large size of the K cation.[27, 28] Meanwhile, $NaNbO_3$ has the anti-ferroelectric property at room temperature because of the small ionic radius of Na.[29] Therefore, a small addition of $KNbO_3$ to $NaNbO_3$ produces a ferroelectric phase. Moreover, the $K_{0.5}Na_{0.5}NbO_3$ (NKN) composition is close to the morphotropic phase boundary (MPB) between two orthorhombic phases, thereby resulting in more polarization directions (a total of 12 directions along orthorhombic [110] axes) and a highly ferroelectric character.[30, 31]

The crystalline structure and morphology of the $K_xNa_{1-x}NbO_3$ powders were investigated. As shown in Fig. 2a, the structures of both $NaNbO_3$ and $KNbO_3$ were identified as orthorhombic. (Full-range data are provided in Fig. S1, supporting information.) At $0.45 < x < 0.9$ in the $K_xNa_{1-x}NbO_3$ system, the observed diffraction peaks shifted from those associated with $KNbO_3$ to those associated with $NaNbO_3$ as Na was added, indicating that a solid solution was well formed over the entire range of composition. Fig. 2b displays an SEM image of typical NKN powder. The average size of the NKN powder was estimated to be 1.5 μm, and the particles exhibited regular polyhedral morphology. All solid-solution samples have similar dimension (about 1~2 μm) and morphology (Fig. S2). Moreover, the specific surface area of $K_xNa_{1-x}NbO_3$ solid-solution samples ranged from 0.3 to 0.8 m^2 g^{-1}, indicating the micro-size powders (Table S1). Using the Rietveld analysis, NKN was found to have a monoclinic structure with the following lattice parameters: a = 8.001 Å, b = 7.882 Å, c = 7.993 Å and β = 90.3°.

To fabricate polarized powders directly, the corona-poling method was adopted. Conventionally, polarized powder has been obtained by grinding sintered pellets in directly contact with a DC voltage under a silicone oil bath. However, this approach results in a decrease of the remanent polarization because of friction forces between the particles; it has been confirmed that the HER activity of conventionally polarized powder increases only a little (Fig. S3). Stress-induced polarization reduction via domain formation is readily possible in all ferroelectrics, especially free-standing particles. Therefore, we adopted the well-known corona-poling method, which has the advantage of being a non-contact method and is known to be applicable for various substances such as films and polymers, as a powder poling method for the first time.

Fig. 3a illustrates the lab-made corona-poling system modified for inducing polarity in powders. This system primarily consists of two electrodes: one is designed with a sharp-cornered shape (corona needle), and the other is designed with a smooth, large-diameter rounded shape (Cu disk). When the electric field is applied on the needle electrode, the electric-field intensity around the sharp point becomes much higher than it is elsewhere and strong enough to ionize a neutral fluid (air); accordingly, a plasma composed of positive ions and free electrons is formed. These charged particles are separated from each other by the electric field, and the separated electrons collide with other atoms/molecules, producing further electron/positive-ion pairs, which then continue to repeat this

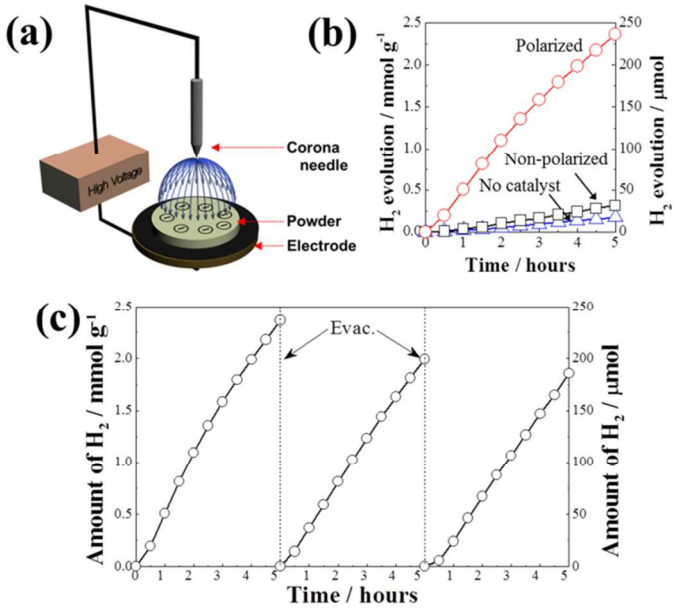

Fig. 3 (a) Illustration of the corona-poling system. (b) Amount of hydrogen evolution for polarized and non-polarized $Na_{0.5}K_{0.5}NbO_3$ powder under UV-light irradiation. The experiment of aqueous methanol solution without any photocatalysts was also carried out. (c) Temporal profile of H_2 evolution for polarized $Na_{0.5}K_{0.5}NbO_3$ powder. The gas phase was evacuated every 5 h after startup.

process. If the needle electrode is more negative than the disk electrode, the ions are attracted to the needle, and the electrons are repelled to the disk (negative corona), inducing a negative charge on the upper surface of the material.[32] In this study, the NKN powder was laid on the copper plate and polarized by the negative corona discharge. Then, we obtained the polarized sample in powder form without mechanically breaking the pellet.

The photocatalytic HER activity of the NKN powders before and after polarization was examined under UV-light irradiation. As shown in fig. 3b, the H_2 evolution rate of the polarized NKN powder was ~0.47 mmol g^{-1} h^{-1}, which was 7.4 times higher than that of the non-polarized NKN powder (~63 μmol g^{-1} h^{-1}). Small amount of hydrogen gas (34 μmol g^{-1} h^{-1}) was observed from only an aqueous methanol solution, which is ascribed to photochemical H_2 evolution by high power (450 W) of UV light.[33] To exclude the photochemical reaction, we carried out the same measurement under a 300 W xenon-arc lamp (Fig. S4). No H_2 evolution was observed under only an aqueous methanol solution, indicating that the majority of the H_2 evolution is caused by photocatalytic reactions. Moreover, the HER rate of NKN powder (13 μmol g^{-1} h^{-1}) is similar to previously reported value.[33] It is noted that polarized NKN powder also showed the higher photocatalytic activity (40 μmol g^{-1} h^{-1}) than non-polarized one under Xe lamp irradiation. Furthermore, at 320 nm, polarized NKN loaded with 1 wt% Pt recorded higher apparent quantum yields (3.9%) than the non-polarized one loaded with 1 wt% Pt (2.4%). Note that rate of increase by polarization was diminished when Pt co-catalyst loaded; it may imply that polarization effect plays a similar role with Pt co-catalyst in charge separation. Fig. 3c shows that the HER activity of the polarized NKN powder was still greater than 80% after reuse in three cycles for a total of 15 h, confirming the good stability of the polarized NKN powder. Moreover, the turnover number, the ratio of the number of reacted electrons to the amount of surface Nb, was estimated to be 890 for 15 h. Therefore, it was clearly demonstrated that the HER activity in the PS system was enhanced by the polarization field.

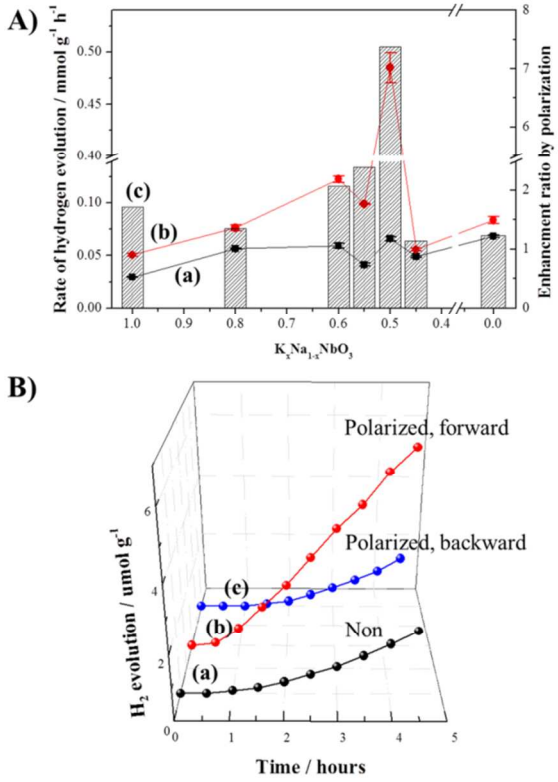

Fig. 4 A) Rate of hydrogen evolution for $Na_{1-x}K_xNbO_3$ solid-solution powders (a) before and (b) after corona poling. (c) Enhanced photocatalytic HER activity ratio of polarized powder to non-polarized powder. B) Amount of hydrogen evolution for (a) non-polarized and (b-c) polarized $Na_{0.5}K_{0.5}NbO_3$ with (b) forward (light exposed to positively charged surface) and (c) backward (light exposed to negatively charged surface) illumination.

To further investigate the effect of polarization in ferroelectric powder on photocatalytic HER, the composition dependence of the HER activity of the $K_xNa_{1-x}NbO_3$ powders before and after polarization was analyzed (Fig. 4A). Each experiment was conducted over an interval of 5 hours under UV irradiation, and the points in the figure were estimated via linear-regression analysis; the error bars represent the standard deviation of the average measurement value. The polarization-enhancement ratio was defined as the activity ratio between the polarized powder and the non-polarized powder. It is clearly shown that the ratio sharply increases as x approaches 0.5, and it reaches its maximum value at x=0.5. This data trend seems to be in good agreement with the behavior of the polarized field strength as a function of composition as shown in Fig. 1c. Thus, the local maximum at x = 0.5 are consistent with the composition dependence of the polarization, demonstrating a positive correlation between the strength of the polarization field and the enhancement ratio of HER activity. However, some points (x =0, 1) are not consistent with the above discussion: $NaNbO_3$ and $KNbO_3$ are also enhanced by corona poling even though the P_r vale is almost 0; it implies that secondary factors should be considered. Another factor that can affect the HER activity is change of the exposed surface via the corona discharge. The difference between the corona poling and the conventional method using two parallel electrodes is that the corona poling may inject a large amount of electrons into the sample. Hence, these injected electrons could form space charge layers inside the particles and induce a change of the exposed surface. Similar surface chemical modification has been shown to change the photoactivity, either through the introduction of defects,

dopants, or etc.[34] Thus, the increase of the HER activity can also be attributed to change of the exposed surface by corona poling. The trend in the end point (x = 0, 1) for the $K_xNa_{1-x}NbO_3$ can be explained in this manner. The photocatalytic performance is also affected by many factors, including the surface area, microstructure, morphology and optical characteristics. Over the whole range of the solid-solution composition, it was confirmed that microstructure and morphology is similar, and also absorbance and band gap is within a similar extent (see Fig. S2 and S5).

These results demonstrate that the enhancement of HER activity in ferroelectric powder caused by polarization can be mainly attributed to the internal dipole field. After the poling process, a permanent internal electric field is generated in the powder by the remanent polarization (Fig. 1a). When the powder is irradiated with light and electrons and holes are photogenerated, the internal field promotes the separation of the electrons and holes. Moreover, the separated electrons are accumulated on the positive surface by the electric field. Therefore, the remanent polarization assists in the increase of the photocatalytic HER activity in the powder.

As another piece of evidence, the effect of the polarization direction on the HER activity was observed in a sintered NKN pellet under UV irradiation (see Fig. 4B). To exclude the possibility of surface change via corona discharge, conventional poling method using two parallel electrodes was adopted; the pellet was poled under 3 kV mm^{-1} bias in a silicone oil bath. For the photocatalytic hydrogen evolution reaction (HER), the UV light was exposed to the (+) and (-) NKN surfaces; this was defined as *forward* and *backward* illumination, respectively. As shown in Fig. 4B, enhanced HER under *forward* illumination was observed after poling. In contrast, the HER after poling under *backward* illumination was nearly the same as that of a non-polarized NKN pellet. As UV photons penetrate to a depth of 1 μm,[35] the transport of photoinduced charges to the opposite side of the pellet can be excluded. Thus, it was confirmed that the activity increased only on the (+) surface, but there was no effect on the (-) surface, implying that the (+) surface plays an essential role in assisting the photocatalytic HER. The improved HER activity on the (+) NKN surface is attributed to the higher charge separation caused by the ferroelectric photovoltaic (FPV) effect. Because the photovoltage is one order of magnitude higher than the band gap of the material in polarized powders, electrons generated from the bulk region can be transported to the positively charged surface, which is similar to an additional bias effect. Inoue et al. have reported that polarization fields increase the HER activity of electrons on a positively charged surface via the FPV effect.[15] In addition, the improved activity on the (+) NKN surface can be interpreted as an effect of efficient charge transfer via band bending. Because NKN is an n-type material, a Schottky barrier (or upward band bending) is formed throughout the interface between powder and water, retarding the electron transfer to the water. However, internal electric fields induce the downward bending of bands on the positive surface and the upward bending of bands on the negative surface. Thus, electron and holes can be easily transferred to the electrolyte on the positive and negative surfaces, respectively. Some have reported the photochemical behavior on the positively charged surface and interpreted it in terms of band structure. Cheong et al. have suggested that the Schottky-barrier height is reduced and that oxygen vacancies accumulate on the positively charged surface,[16] promoting the charge transfer of photogenerated electrons to the electrolyte. Additionally, Rohrer et al. have proposed that the polarization for the positive domain reduces the upward band bending generated at the interface between semiconductor and electrolyte. Thus, bands may be bent downward, facilitating the charge transfer to the electrolyte.[36, 37] Therefore, the improved HER activity on the (+) NKN surface is attributed to the improvement in the charge-separation property caused by the photovoltaic effect and the efficient charge-transfer characteristic promoted by band bending.

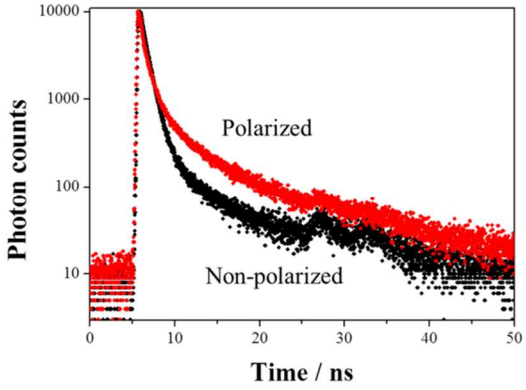

Fig. 5 Decay profile of photoluminescence from $K_{0.5}Na_{0.5}NbO_3$ powders before and after corona poling

In order to demonstrate this advantage of polarization more directly, time-resolved photoluminescence (PL) lifetime measurements were performed. As shown in Fig. 5, the electrons that were excited in polarized NKN have the longer life time than non-polarized one. PL decay profiles could be analyzed by multi-exponential fitting models as following equation.[38]

$$\mathbf{I(t)} = \sum \boldsymbol{A_i e^{-t/\tau_i}} \quad (1)$$

where A_i and τ_i is the amplitude and the life time, respectively. Also, the intensity-average life time, τ_{avg}, could be calculated by following equation.[39]

$$\langle \boldsymbol{\tau} \rangle = \frac{\sum A_i \tau_i^2}{\sum A_i \tau_i} \quad (2)$$

Photoluminescence lifetime and the related parameters of polarized and non-polarized NKN powders are summarized in Table S2. The PL of both polarized and non-polarized NKN powders showed triexponential kinetics and the lifetime for polarized NKN powder was 3.31 ns, which is significantly longer than that of non-polarized one (1.64 ns). This result clearly demonstrates that the internal field can inhibit the charge recombination, promoting the separation of the electrons and holes.[40]

The effect of polarization on the HER activity of nano NKN powder was also investigated. Nano NKN powder was synthesized via the polymeric complex method, consistent with the NKN phase (Fig. S6). The average size of the nano NKN powder was 45 nm, and the particles exhibited cubic morphology (Fig. S7). The H_2 evolution rate of the nano NKN powder before the poling process was 0.06 mmol g^{-1} h^{-1}, but the activity after the poling process remained the same (not shown here). Size limits in ferroelectric photocatalysts were considered in terms of polarization decay. Generally, the polarization field decreases faster at the nanoscale than at the bulk level as the long-range ordering of the dipoles decreases, which is related to the changes in the atomic polarization, non-uniform strain, defect microstructure, and imperfect polarization screening at the surface.[41] Therefore, the decay rate gradually increases with decreasing particle size via a disordering process, implying that photocatalytic HER activity at the nanoscale cannot be assisted by the polarization effect. Time-dependent polarization decay can be interpreted as the dynamics of ferroelectric-domain decay. The

dependence of the domain lifetime can be calculated based on the initial domain radius as follows:[42]

$$\tau(r) = \tau_0 \exp\left[\alpha\left\{\left(\frac{r}{R_C}\right)^{3/2} - 1\right\}\right] \qquad (3)$$

where τ is the lifetime, r is the initial domain radius, and R_C is the critical radius for domain stability. For example, because R_C of $BaTiO_3$ is evaluated to be 74 – 104 nm, domains with the initial radius of 100 nm are only stable about 30 min according to equation (3).[42] Also, $SrBi_2Ta_2O_9$ films showed that domains of radius 75 nm exist only 10 min, whereas domains of radius 95 nm have lifetime 3 orders of magnitude longer; it indicates the existence of a critical radius R_C ~ 85 nm.[43] In this manner, lifetime of nanoparticle of NKN could be evaluated by calculating the R_C value. According to Molotskii et al., R_C is proportional to $1/P_s^{4/3}$ and $1/E_c^{2/3}$.[42] Therefore, R_C of NKN could be simply estimated to be 45 ~ 60 nm from the R_C of $BaTiO_3$ by using P_s (14.7 μC cm^{-2}) and E_c (14.0 kV cm^{-1}) of NKN. It implies that polarization of NKN nanoparticles with a diameter not exceeding 50 nm may decay rapidly after removing the external field. This is why the nano NKN powder with a size of 45 nm was observed to have the same HER activity before and after polarization. Thus, it is thought that a trade-off exists between maintaining the polarity and enlarging the surface area of such a material. Further research is ongoing to determine the optimum size for achieving superior catalytic activity via both a high polarity and a large surface area.

Conclusions

The proposed polarized $K_{0.5}Na_{0.5}NbO_3$ powder prepared via a simple corona-poling method proved to be an effective ferroelectric photocatalyst for H_2 evolution in a particulate-suspension system. The activity-enhancement ratio of a $K_xNa_{1-x}NbO_3$ solid solution is dependent on the composition and size. The positively charged surface clearly plays an essential role in promoting the photocatalytic activity. Under optimal conditions, the photocatalytic activity of the $K_{0.5}Na_{0.5}NbO_3$ powder increased by up to a factor of 7.4. Furthermore, we envisage that the corona-poling procedure can be expanded to achieve powder polarization for the enhancement of the activity of photocatalysts in other fields, such as pollutant decomposition, CO_2 reduction, etc. We believe that it can open a new avenue of exploration and design for a variety of particle-based catalysts with ferroelectric properties for the attainment of efficient catalytic performance.

Acknowledgements

This work was supported by the Global Frontier R&D Program on Center for Multiscale Energy System (2011-0031574), Basic Science Research Program (2012-0004117), institutional research program of the Korea Institute of Science and Technology (2E24001), and Mid-Career Researcher Program (2012-0008669, RIAM) funded by the National Research Foundation under the Ministry of Education, Science and Technology, Korea.

Notes and references

[a] *Department of Materials Science and Engineering, Seoul National University, Seoul 151-744, Korea. E-mail: kshongss@plaza.snu.ac.kr; nkitae@snu.ac.kr; Tel: +82-2-880-7165*
[b] *Korea Institute of Science and Technology, Seoul 136-130, Korea.*
[c] *KU-KIST Graduate School of Converging Science and Technology, Korea University, Seoul 136-701, Korea.*

† Electronic Supplementary Information (ESI) available: experimental details; XRD (Fig. S1), SEM (Fig. S2) and UV-vis (Fig. S5) results of the solid-solution powders; Additional hydrogen evolution measurements (Fig. S4-5); XRD and SEM of the NKN nano powder (Fig. S6-7). See DOI: 10.1039/c000000x/

1 M. Kitano and M. Hara, *J. Mater. Chem.*, 2010, **20**, 627-641.
2 H. Zhang, G. Chen and D. W. Bahnemann, *J. Mater. Chem.*, 2009, **19**, 5089-5121.
3 H. Kato, K. Asakura and A. Kudo, *J. Am. Chem. Soc.*, 2003, **125**, 3082-3089.
4 K. Maeda, K. Teramura, D. Lu, T. Takata, N. Saito, Y. Inoue and K. Domen, *Nature*, 2006, **440**, 295.
5 K. Maeda, T. Takata, M. Hara, N. Saito, Y. Inoue, H. Kobayashi and K. Domen, *J. Am. Chem. Soc.*, 2005, **127**, 8286-8287.
6 F. E. Osterloh, *Chem. Mater.*, 2007, **20**, 35-54.
7 A. Kudo and Y. Miseki, *Chem. Soc. Rev.*, 2009, **38**, 253-278.
8 H. Tong, S. Ouyang, Y. Bi, N. Umezawa, M. Oshikiri and J. Ye, *Adv. Mater.*, 2012, **24**, 229-251.
9 Z. Li, W. Luo, M. Zhang, J. Feng and Z. Zou, *Energ. Environ. Sci.*, 2013, **6**, 347-370.
10 X. Chen, S. Shen, L. Guo and S. S. Mao, *Chem. Rev.*, 2010, **110**, 6503-6570.
11 S. W. Seo, S. Park, H. Y. Jeong, S. H. Kim, U. Sim, C. W. Lee, K. T. Nam and K. S. Hong, *Chem. Comm.*, 2012, **48**, 10452-10454.
12 X. Yang, X. Su, M. Shen, F. Zheng, Y. Xin, L. Zhang, M. Hua, Y. Chen and V. G. Harris, *Adv. Mater.*, 2012, **24**, 1202-1208.
13 V. M. Fridkin and B. Popov, *Sov. Phys. Uspekhi*, 1978, **21**, 981-991.
14 P. S. Brody and F. Crowne, *J. Electron. Mater.*, 1975, **4**, 955-971.
15 Y. Inoue, *Energ. Environ. Sci.*, 2009, **2**, 364-386.
16 H. T. Yi, T. Choi, S. G. Choi, Y. S. Oh and S. W. Cheong, *Adv. Mater.*, 2011, **23**, 3403-3407.
17 N. V. Burbure, P. A. Salvador and G. S. Rohrer, *Chem. Mater.*, 2010, **22**, 5823-5830.
18 J. L. Giocondi, G. S. Rohrer, *J. Phys. Chem. B*, 2010, **105**, 35, 8275-8277 (2001)
19 Y. Inoue, K. Sato and K. Sato, *J. Chem. Soc., Faraday Trans. 1*, 1989, **85**, 1765-1774.
20 Y. Cui, J. Briscoe, and S. Dunn, *Chem. Mater.,* 2013, **25**, 4215−4223.
21 G. Li, Z. Yi, Y. Bai, W. Zhang and H. Zhang, *Dalton Trans.*, 2010, **41**, 10194-10198.
22 L. Jiang, Y. Zhang, Y. Qiub and Z. Yi, *RSC Adv.*, 2014, **4**, 3165-3170.
23 M. Pattanaik, Ph. D. Thesis, National Institute of Technology, 2011
24 S. Huo, S. Yuan, Z. Tian, C. Wang, Y. Qiu and C. Randall, *J. Am. Ceram. Soc.*, 2012, **95**, 1383-1387.
25 H. J. Liu, B. P. Zhang, J. F. Li and K. Wang, *Key Eng. Mat.*, 2007, **336**, 224-227.
26 J. B. Lim, S. Zhang, J.-H. Jeon and T. R. Shrout, *J. Am. Ceram. Soc.*, 2010, **93**, 1218-1220.
27 D. J. Singh and L. L. Boyer, *Ferroelectrics*, 1992, **136**, 95-103.

28 L. A. Bugaev, K. N. Zhuchkov, V. A. Shuvaeva, E. B. Rusakova, *Jpn. J. Appl. Phys.*, 1999, **38**, 215-217.
29 S.-Y. Chu, W. Water, Y.-D. Juang and J.-T. Liaw, *Ferroelectrics*, 2003, **287**, 23-33.
30 Y.-J. Dai, X.-W. Zhang and K.-P. Chen, *Appl. Phys. Lett.*, 2009, **94**, 042905.
31 J. Fu, R. Zuo, X. Wang and L. Li, *J. Phys. D Appl. Phys*, 2009, **42**, 012006.
32 F. W. Peek, *Dielectric phenomena in high voltage engineering*, McGraw-Hill Book Company, Inc., New York, NY, 1920.
33 K. Saito and A. Kudo, Inorg. Chem., 2010, **49**, 2017-2019.
34 H. Park, Y. Park, W. Kim and W. Choi, *J. Photoch. Photobio. C*, 2013, **15**, 1-20.
35 M. Razeghi and A. Rogalski, *J. Appl. Phys.*, 1996, **79**, 7433-7473.
36 N. V. Burbure, P. A. Salvador and G. S. Rohrer, *Chem. Mater.*, 2010, **22**, 5831-5837.
37 A. Bhardwaj, N. V. Burbure, A. Gamalski and G. S. Rohrer, *Chem. Mater.*, 2010, **22**, 3527-3534.
38 G. Williams and P. V. Kamat, *Langmuir*, 2009, **25**, 13869–13873.
39 Y.-C. Chen, Y.-C. Pu and Y.-J. Hsu, *J. Phys. Chem. C*, 2012, **116**, 2967-2975.
40 H. J. Yun, D. M. Lee, S. Yu, J. Yoon, H.-J. Park, and J. Yi, *J Mol. Catal. A-Chem.*, 2013, **378**, 221-226.
41 P. M. Rorvik, T. Grande and M. A. Einarsrud, *Adv. Mater.*, 2011, **23**, 4007-4034.
42 M. I. Molotskii and M. M. Shvebelman, *J. Appl. Phys.*, 2005, **97**, 084111.
43 A. Gruverman and M. Tanaka, *J. Appl. Phys.* 2001, **89**, 1836-1843.

Table of Content entry

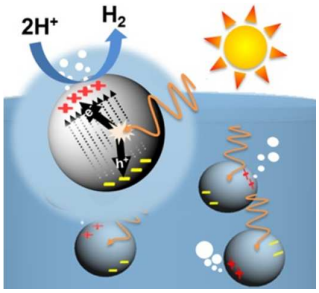

Dramatically improved hydrogen evolution activity in a particulate-suspension system is demonstrated for $K_{0.5}Na_{0.5}NbO_3$ powder polarized via simple corona poling, providing a key guideline for imposing an electric field on a ferroelectric photocatalyst.